

## Slope stability analysis along the proposed Kathmandu–Hetauda Road with tunnel sections

I. R. Humagain<sup>1</sup>, K. Schetelig<sup>1</sup>, M. P. Sharma<sup>2</sup>,  
B. N. Upreti<sup>3</sup>, and M. Langer<sup>4</sup>

<sup>1</sup>Department of Engineering Geology and Hydrogeology in Aachen University of Technology,  
Lochner Str. 4 - 20, D-52056 Aachen, Germany

<sup>2</sup>Tribhuvan University Central Office, Kirtipur, Kathmandu, Nepal

<sup>3</sup>Department of Geology, Tri-Chandra Campus, Tribhuvan University, Ghantaghar, Kathmandu, Nepal

<sup>4</sup>Bundesanstalt fuer Geowissenschaften und Rohstoffe (BGR), Stilleweg - 2, D-30655 Hannover, Germany

### ABSTRACT

The proposed Kathmandu-Hetauda Road alignment passes through Thankot, Chitlang, Kulekhani, Bhimpheedi, and Bhaisedobhan. It is the shortest as well as least hazardous route very suitable for a standard highway. It has the following three tunnel sections: the Thankot Tunnel (3.2 km long), the Kulekhani Tunnel (500 m long), and the Chisapani Tunnel (3.8 km long). The alignment passes through the Kathmandu Nappe, Upper Nawakot Group of the Lesser Himalaya, and the Siwaliks. It also crosses the Main Boundary Thrust and the Mahabharat Thrust, four major faults/shear zones, and a major fold axis.

The areas of plane sliding, wedge sliding, and toppling are delimited on the basis of the study of discontinuities along the proposed alignment. The stability analysis shows that 60–75% of the total road length is stable, 20–30% is fair, 5–15% is weak, and 2–5% is critical.

### INTRODUCTION

Altogether five alternative routes were proposed to the HMG of Nepal by various consultants (e.g., FINNIDA 1993) for the construction of a direct road link between Kathmandu, the capital of Nepal, and Hetauda town (Fig. 1). Each of the proposed alignments crosses the geological units of the Kathmandu Nappe (Hagen 1969; Upreti and Le Fort 1997), the Upper Nawakot Group (Stöcklin and Bhattarai 1977; Stöcklin 1980) of the Lesser Himalaya as well as the Siwaliks (Fig. 2). The alignments cross the Main Boundary Thrust (MBT), the Mahabharat Thrust (MT), four major faults/shear zones, fifteen local faults/shear zones, and a number of small-scale faults/shear zones.

After the prefeasibility study, the consultants suggested the following two alternative alignments for consideration: 1) the 59 km double-lane road: Kathmandu–Chandragiri and Chisapani Tunnels– Bhainse – Hetauda; and 2) the 64 km double-lane road: Kathmandu–Bagmati River– Kulekhani–Chisapani Tunnel–Bhainse – Hetauda. Out of these two, the first alignment was considered to be the most feasible and was recommended for the detailed study.

The first alignment follows essentially a portion of the ancient route linking India and Tibet for over two thousand years. The geotechnical studies carried out along this most feasible alignment are described below. This alignment will be shorter by 70% as compared to the existing Tribhuvan Highway (Kathmandu–Hetauda Road) and will reduce the travel time from 6–8 hours to only 1–2 hours.

### GEOTECHNICAL STUDY ALONG THE MOST FEASIBLE ALIGNMENT

The alignment follows the gently sloping valley of the Chitlang Khola. The rocks are gently dipping due SSW or NNE and form a syncline (Fig. 3). This section crosscuts about 10 weak zones (faults, thrusts, and shear zones). The Kulekhani section of the alignment passes through the steep left bank of the Kulekhani Reservoir. The foliation is generally parallel to the bedding and dips at 33–50° due NNE. This section of the road crosscuts 3 faults/shear zones (Fig. 4). While following the existing Bhimpheedi–Bhainse Road along the Rapti Khola Valley, the section passes mainly through rock and partly through colluvial or alluvial soil slopes. The rocks are intensely deformed owing to the intrusion of granite (Fig. 5). The foliation is dipping at 33–70° due SSW and NNE forming synclines and anticlines. Altogether eight axial traces of fold extend due east–west in this section of the alignment. This section of the road crosscuts seven faults/shear zones.

While following the Tribhuvan Highway, the Bhainse–Hetauda section of the proposed alignment passes through the rocky slope on the left bank of the Rapti Khola. The rocks dip at moderate to high angles towards the north. The foliation of the metamorphic sequence dips steeply towards NNE. This road section crosscuts four faults/shear zones including the MBT and MT (Fig. 6).

#### Rock mass

Medium- to fine-grained, soft to moderately hard, greenish grey mudstone, shale, chert, sandstone, limestone,

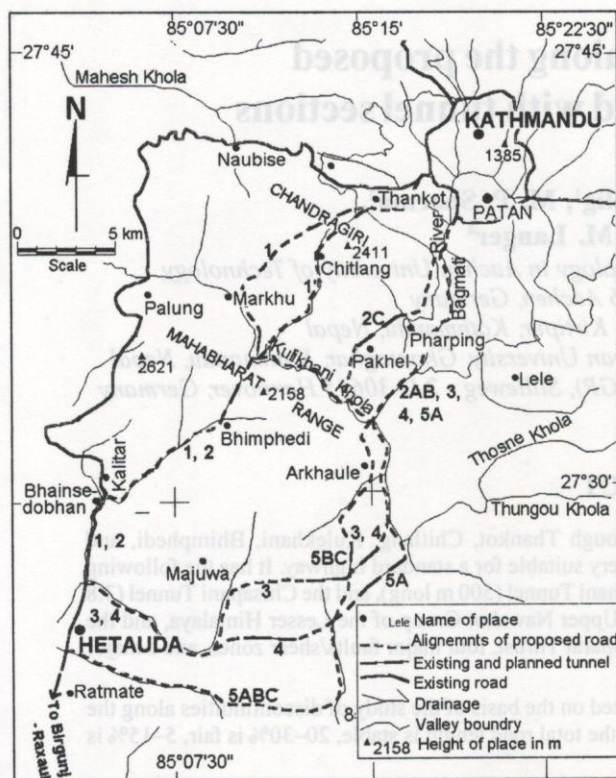


Fig. 1: The alternative routes for the Kathmandu – Hetauda direct road link, proposed by FINNIDA (1993)

and calcareous phyllite are the main rock types in the Chitlang section. Phyllite, calcareous phyllite, limestone, and marble are the main rocks in the Kulekhani section. The Bhimphedi-Bhainsedobhan section lies in the garnetiferous schist, quartzitic schist, micaceous quartzite, white quartzite, and marble. Such rocks as marble, garnetiferous schist, phyllite, quartzite, slate, argillaceous dolomite, conglomerate, sandstone, and mudstone are exposed in the Bhainsedobhan-Hetauda section.

Four close to very close sets of discontinuity (i.e. a foliation or bedding joint set, two preferred joint sets, and one random joint set) are prominent. The discontinuity surfaces in quartzite and sandstone are rough, and open, whereas those of phyllite, mudstone, shale, schist, and garnetiferous schist are relatively smooth, altered, sometimes mineralised, and partly filled with fines. The discontinuity surfaces of limestone and marble are relatively rough, open, sometimes mineralised, and filled with calcareous minerals. The discontinuities along the major thrusts or shear zones (e.g., the Kulekhani Fault, Rapti Khola Fault, MT, and MBT) are frequently slickensided and filled either with clay or siliceous and calcareous minerals.

Following Bieniawski (1976), the rock mass rating (RMR) was carried out along the proposed alignment on the basis of the estimated and measured rock mass data (Tables 1, 2, 3,

and 4). Based on the RMR values, the rock mass deformability ( $E_m$ ), cohesion ( $c$ ), and friction angle ( $j$ ) were estimated (Tables 1, 2, 3, and 4). The RMR values in all the sections were found to be  $< 50$ , indicating fair to very weak quality of the rock mass.

**Slope stability analysis**

Slope stability conditions of the Chitlang Valley section, Kulekhani Valley section, Bhimphedi-Bhainse section, and Bhainse-Hetauda section are described below.

*Chitlang Valley section*

The existing fair-weather road passes along a very gently sloping section of the Chitlang Valley. The gently sloping colluvial slopes are composed of the slide and fall debris (GM and GC types of soil according to the Unified Soil Classification System; Wagner 1957) whereas the alluvial slopes are represented by sandy gravel (GS) and silty gravel (GM). The factor of safety ( $FS$ ) with respect to sliding (except the instability due to the surface erosion during monsoon) for such non-cohesive soil was worked out using the following expression.

$$FS = \frac{\tan \phi}{\tan \beta}$$

where  $\phi$  and  $\beta$  are the internal friction and slope angle respectively.

The cut slopes with non-cohesive soil are stable, irrespective of their height as long as the slopes are equal to the lower limit of the angle of internal friction and are suitably drained. Cut slopes of  $30^\circ$  to  $40^\circ$  are mostly stable in the section with non-cohesive soil. In the section with cohesive soil (mainly the residual soil as well as the soil of the central part of the Chitlang Valley containing a higher amount of clay and humus), the stability of cut slope depends on shear parameters ( $c, \phi$ ) of the soil, angle of slope ( $\beta$ ), and the cut slope height ( $H$ ). The critical height of cut slope for cohesive soil was calculated as under:

$$H = \frac{4c}{9.8\gamma}$$

where  $c$  is cohesion and  $\gamma$  is unit weight of soil.

The stability analysis of the slopes containing cohesive soils shows that the slopes of  $30-45^\circ$  are mostly stable, but at some places, the angle of cut slope may have to be decreased to about  $20^\circ$  in order to achieve the required factor of safety.

There are some steep rocky slopes between the Chitlang and Kulekhani Valleys. The rock slope stability analysis indicates that there are two unstable slopes, one likely unstable slope, and six unstable locations if cut slope exceeds  $50^\circ$  (Fig. 3). The slope mass rating (SMR) system (Romana 1985) was applied for this section of the alignment and the results indicate fair to very weak slope stability conditions (Table 1).

*Kulekhani Valley section*

The stability analysis was carried out at 18 exposures, out of which four locations are stable, three are likely

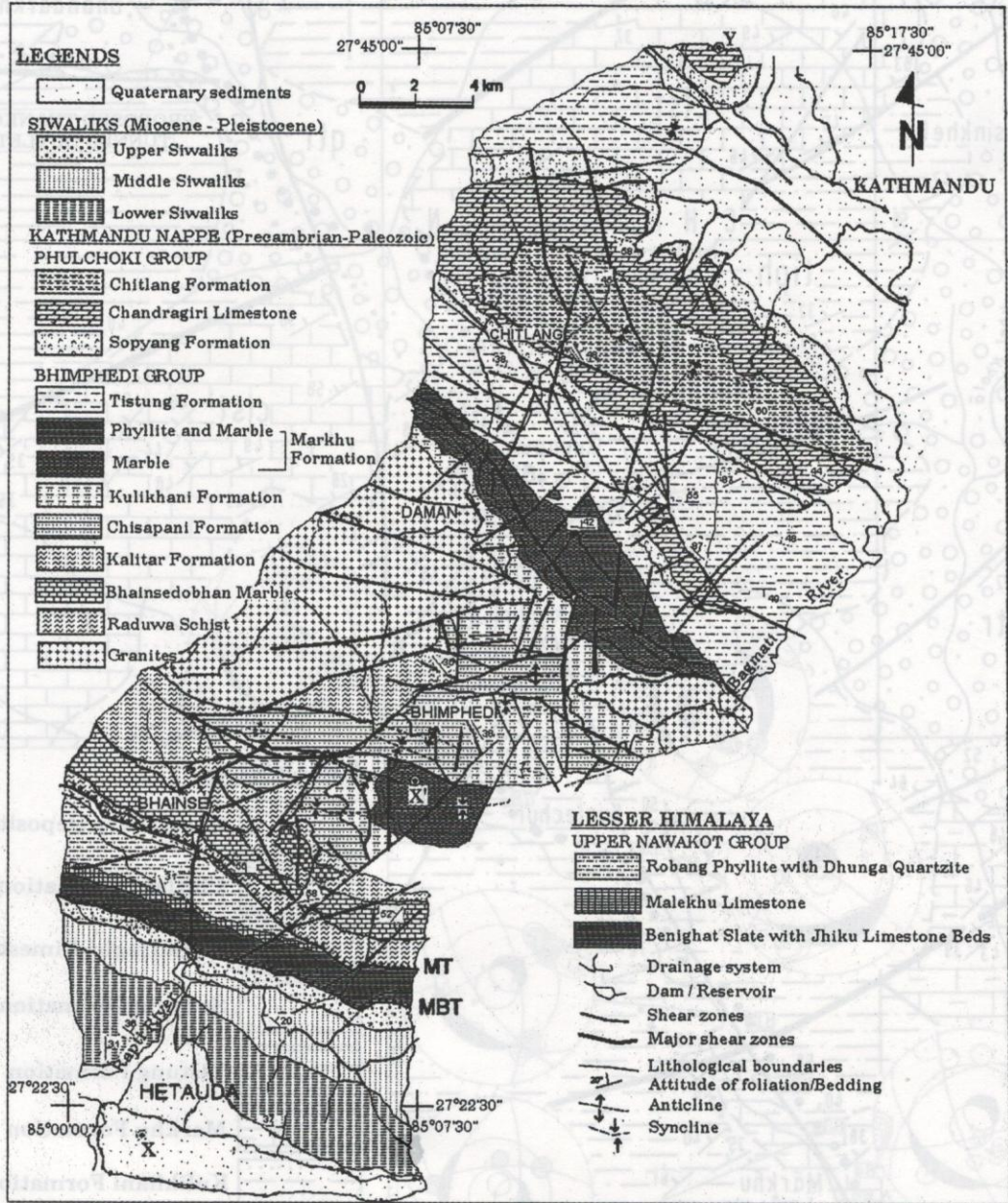


Fig. 2: Geology of the proposed road alignments and cross-section along XX'Y

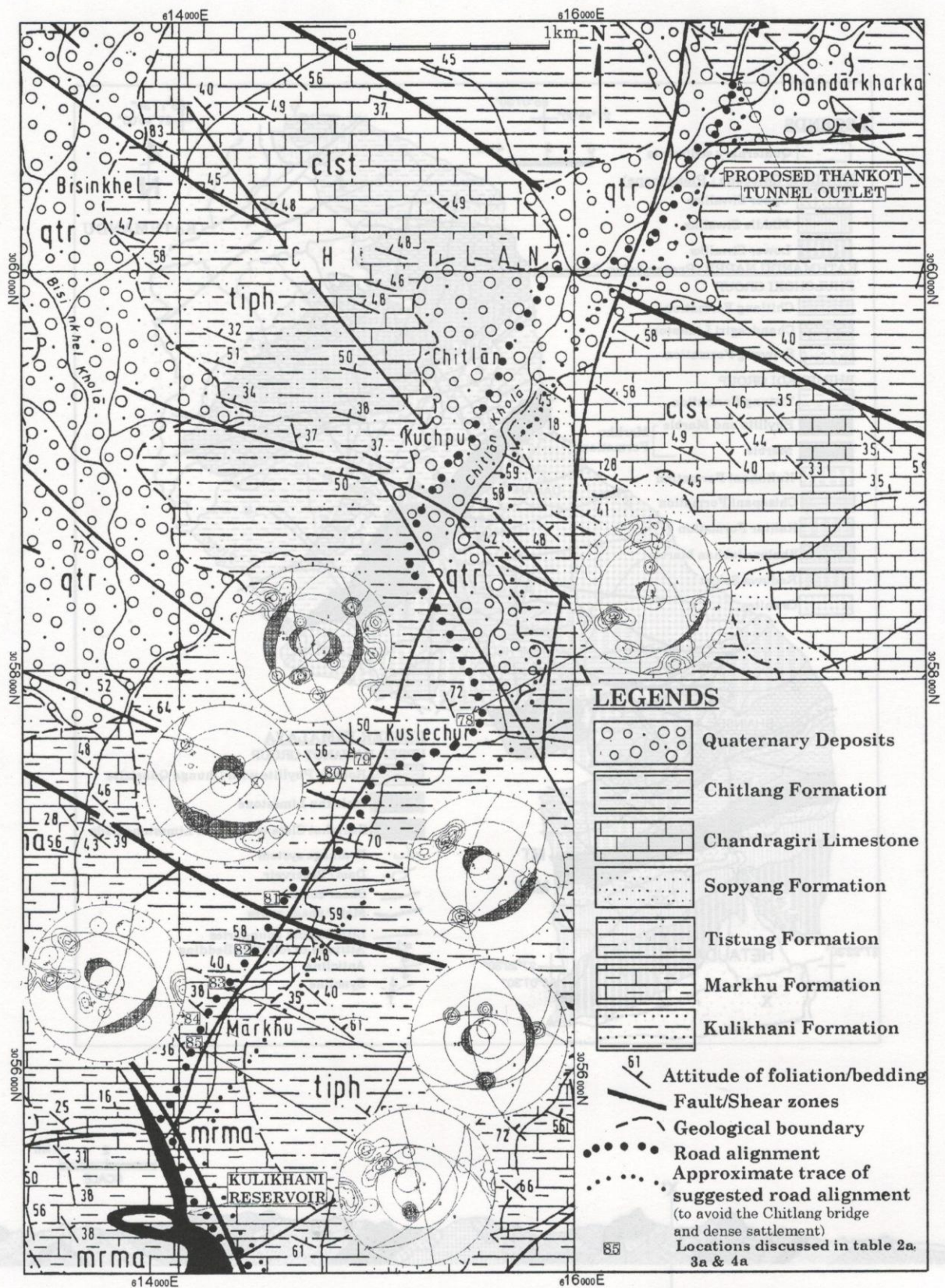


Fig. 3: Engineering geological map of the Chitlang Valley section (the stereographic projection of discontinuities as well as the kinematics of slope stability is also shown).

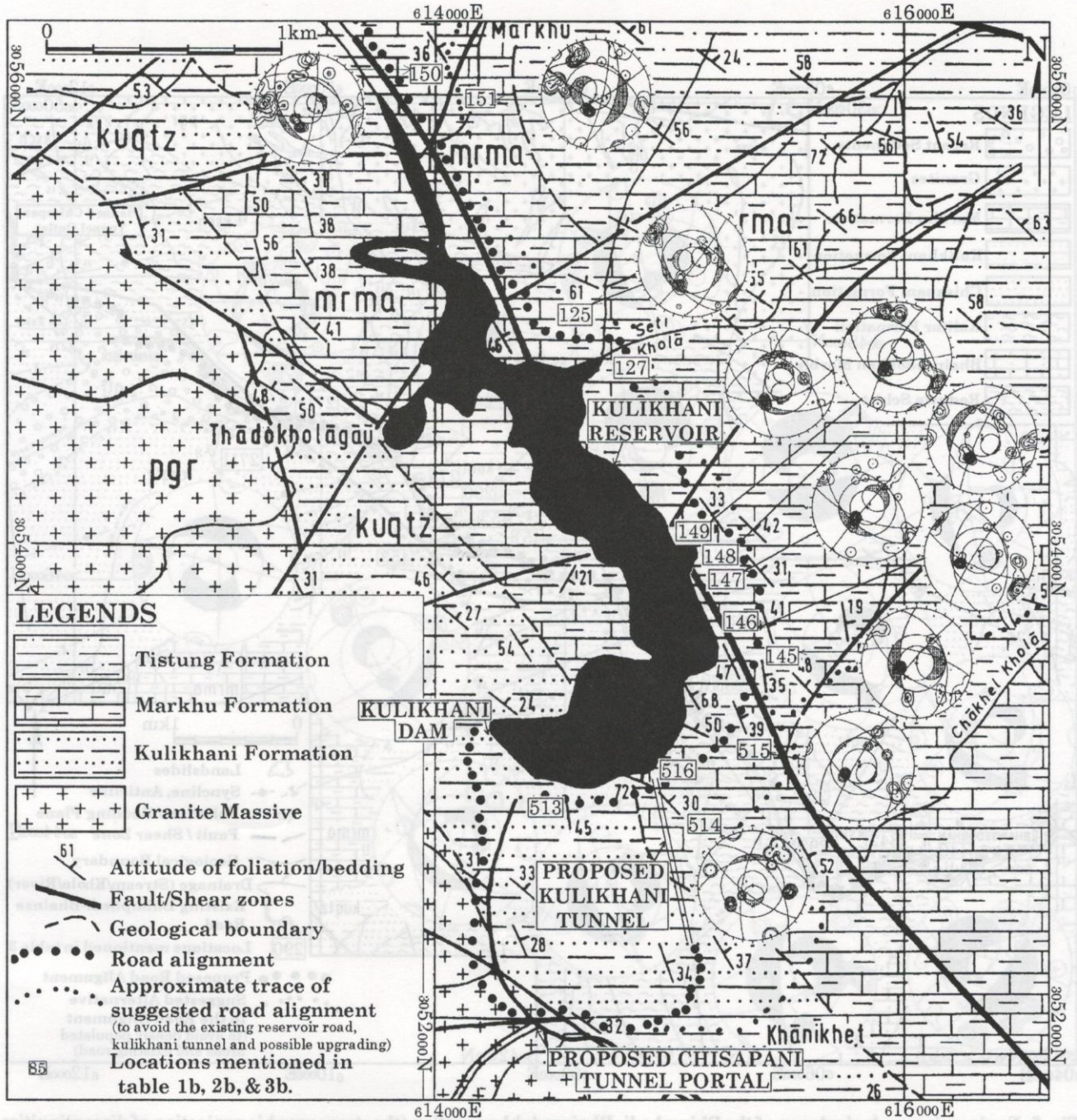


Fig. 4: Engineering geological map of the Kulekhani Valley section (the stereographic projection of discontinuities as well as the kinematics of slope stability is also shown).

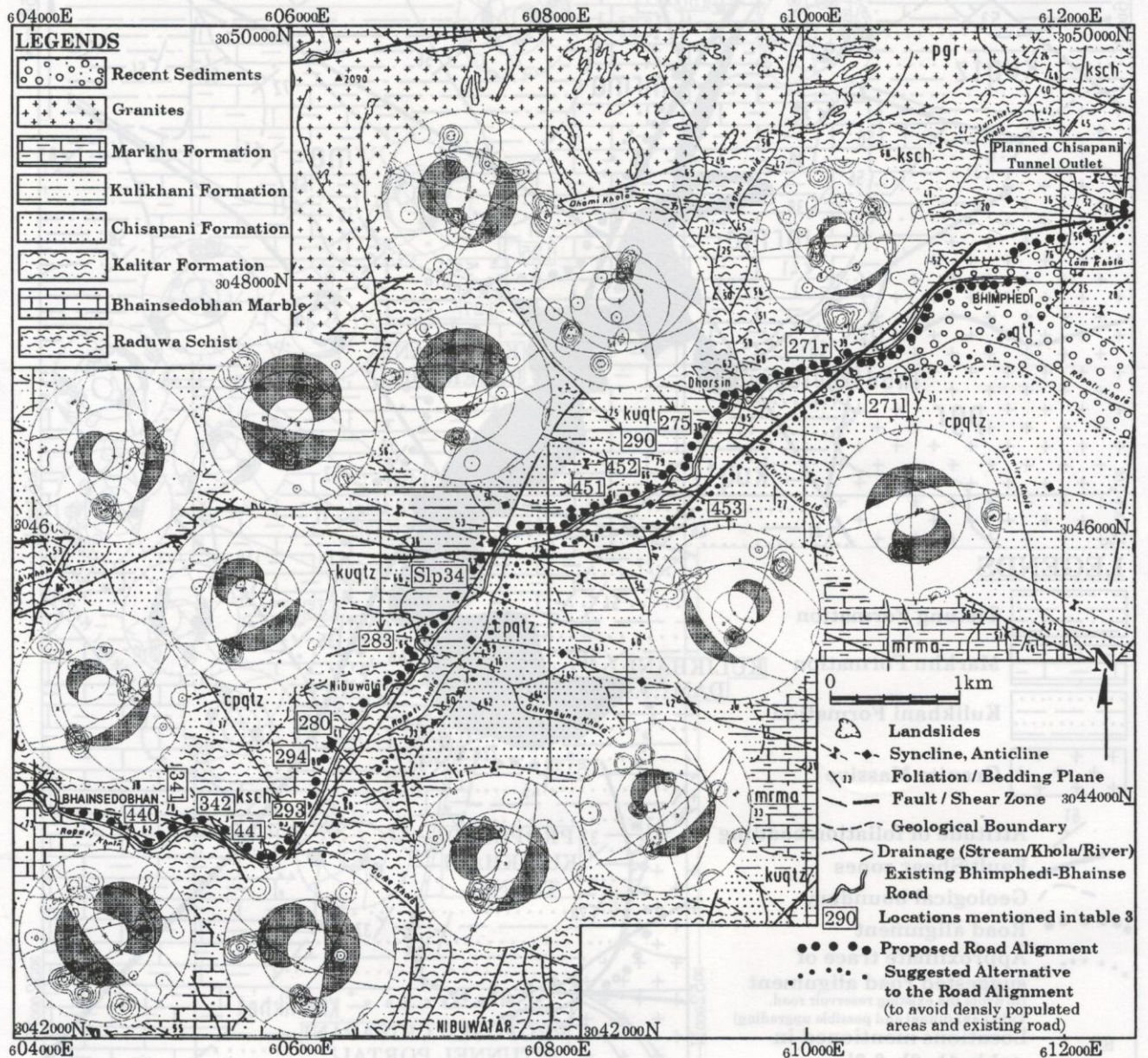


Fig. 5: Engineering geological map of the Bhimpheidi-Bhainsedobhan section (the stereographic projection of discontinuities as well as the kinematics of slope stability is also shown).

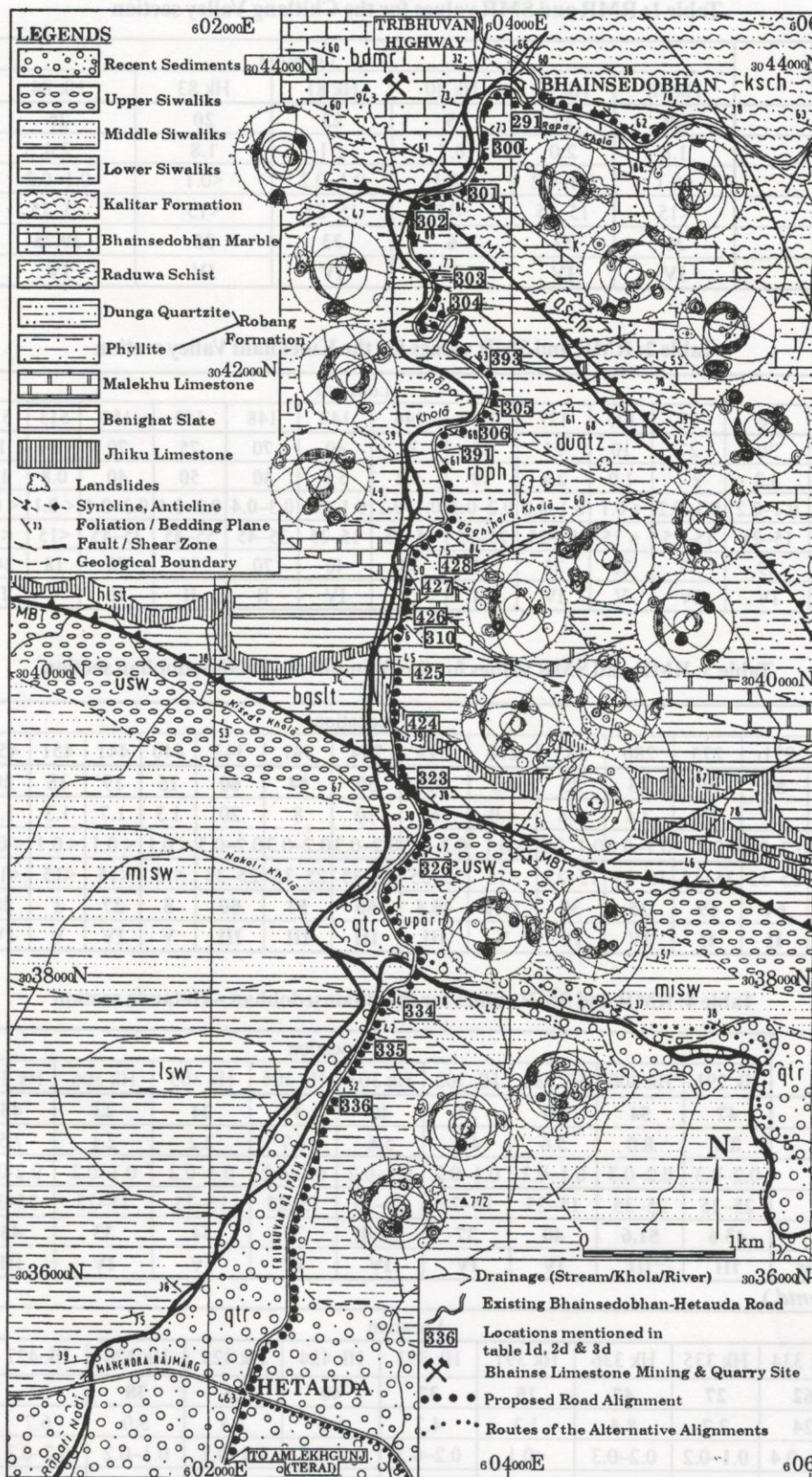


Fig. 6: Engineering geological map of the Bhainsedobhan-Hetauda section (the stereographic projection of discontinuities as well as the kinematics of slope stability is also shown).

**Table 1: RMR and SMR values for the Chitlang Valley section**

Attribute	Location						
	Hk 78	Hk 79	Hk 80	Hk 81	Hk 83	Hk 84	Hk 85
<b>RMR</b>	<b>20</b>	<b>22</b>	<b>5</b>	<b>23</b>	<b>20</b>	<b>25</b>	<b>55</b>
Em	1.8	2.0	0.7	2.1	1.8	2.4	10
C (MPa)	<0.1	0.1–0.2	<0.1	0.1–0.2	<0.1	0.1–0.2	0.2–0.3
$\phi$ (°)	<15	15–25	<15	15–25	<15	15–25	25–35
<b>SMR</b>	<b>30</b>	<b>32</b>	<b>6</b>	<b>33</b>	<b>35</b>	<b>29.75</b>	<b>49.75</b>
<b>Stability class</b>	<b>IV</b>	<b>IV</b>	<b>V</b>	<b>IV</b>	<b>IV</b>	<b>IV</b>	<b>III</b>

**Table 2: RMR and SMR values for the Kulekhani Valley section**

Attribute	Location														
	95	96	97	125	127	145	146	147	148	149	150	513	514	515	516
<b>RMR</b>	<b>35</b>	<b>30</b>	<b>27</b>	<b>10</b>	<b>25</b>	<b>55</b>	<b>35</b>	<b>40</b>	<b>70</b>	<b>75</b>	<b>70</b>	<b>8</b>	<b>15</b>	<b>55</b>	<b>50</b>
Em	4.2	3.2	2.7	1.0	2.4	10	4.2	5.6	40	50	40	0.8	1.3	10	10
C (MPa)	0.1–0.2	0.1–0.2	0.1–0.2	<0.1	0.1–0.2	0.2–0.3	0.1–0.2	0.1–0.2	0.3–0.4	0.3–0.4	0.3–0.4	<0.1	<0.1	0.2–0.3	0.2–0.3
$\phi$ (°)	15–25	15–25	15–25	<15	15–25	25–35	15–25	15–25	35–45	55–45	35–45	<15	<15	25–35	25–35
<b>SMR</b>	<b>45.6</b>	<b>39</b>	<b>37</b>	<b>20</b>	<b>35</b>	<b>55</b>	<b>35</b>	<b>40</b>	<b>70</b>	<b>75</b>	<b>70</b>	<b>18</b>	<b>24.1</b>	<b>55</b>	<b>50</b>
<b>Class</b>	<b>III</b>	<b>IV</b>	<b>IV</b>	<b>V</b>	<b>IV</b>	<b>III</b>	<b>IV</b>	<b>IV</b>	<b>II</b>	<b>II</b>	<b>II</b>	<b>V</b>	<b>IV</b>	<b>III</b>	<b>III</b>

**Table 3: RMR and SMR values for the Bhimpedi – Bhainsedobhan section**

Attribute	Location															
	271l	271r	275	280	283	290	293	294	341	342	440	441	451	452	453	s34
<b>RMR</b>	<b>25</b>	<b>50</b>	<b>59</b>	<b>25</b>	<b>25</b>	<b>10</b>	<b>53</b>	<b>50</b>	<b>54</b>	<b>60</b>	<b>15</b>	<b>19</b>	<b>15</b>	<b>20</b>	<b>45</b>	<b>35</b>
Em	2.4	10	18	2.4	2.4	1.0	6	10	8	20	1.3	1.7	1.3	1.8	7.5	4.1
C (MPa)	0.1–0.2	0.2–0.3	0.2–0.3	0.1–0.2	0.1–0.2	<0.1	0.2–0.3	0.2–0.3	0.2–0.3	0.2–0.3	<0.1	<0.1	<0.1	<0.1	0.2–0.3	0.1–0.2
$\phi$ (°)	15–25	25–35	25–35	15–25	15–25	<15	25–35	25–35	25–35	25–35	<15	<15	<15	<15	25–35	15–25
<b>SMR</b>	<b>35</b>	<b>64</b>	<b>69</b>	<b>35</b>	<b>35</b>	<b>19.1</b>	<b>45.4</b>	<b>50</b>	<b>54</b>	<b>60</b>	<b>5</b>	<b>27</b>	<b>1</b>	<b>28</b>	<b>45</b>	<b>35</b>
<b>Class</b>	<b>IV</b>	<b>II</b>	<b>II</b>	<b>IV</b>	<b>IV</b>	<b>V</b>	<b>III</b>	<b>III</b>	<b>III</b>	<b>III</b>	<b>V</b>	<b>IV</b>	<b>V</b>	<b>IV</b>	<b>III</b>	<b>IV</b>

**Table 4: RMR and SMR values for the Bhainsedobhan – Hetauda section**

Attribute	Location										
	Hk 291	Hk 300	Hk 301	Hk 302	Hk 303	Hk 304	Hk 305	Hk 306	Hk 310	Hk 323	
<b>RMR</b>	<b>47</b>	<b>54</b>	<b>40</b>	<b>37</b>	<b>40</b>	<b>37</b>	<b>24</b>	<b>23</b>	<b>45</b>	<b>15</b>	
Em	8.4	8.0	5.6	4.7	5.6	4.7	2.2	2.1	7.5	1.3	
C (MPa)	0.2–0.3	0.2–0.3	0.1–0.2	0.1–0.2	0.1–0.2	0.1–0.2	0.1–0.2	0.1–0.2	0.2–0.3	<0.1	
$\phi$ (°)	25–35	25–35	15–25	15–25	15–25	15–25	15–25	15–25	25–35	<15	
<b>SMR</b>	<b>43.6</b>	<b>51.6</b>	<b>40</b>	<b>37</b>	<b>36.4</b>	<b>37</b>	<b>34</b>	<b>33</b>	<b>45</b>	<b>25</b>	
<b>Stability class</b>	<b>III</b>	<b>III</b>	<b>IV</b>	<b>IV</b>	<b>IV</b>	<b>IV</b>	<b>IV</b>	<b>IV</b>	<b>III</b>	<b>IV</b>	

(Table 4 contd.)

Location										
Hk 326	Hk 334	Hk 335	Hk 336	Hk 391	Hk 393	Hk 424	Hk 425	Hk 426	Hk 427	Hk 428
<b>34</b>	<b>62</b>	<b>27</b>	<b>47</b>	<b>15</b>	<b>37</b>	<b>40</b>	<b>25</b>	<b>38</b>	<b>43</b>	<b>50</b>
4.0	24	2.7	8.4	1.3	4.7	5.6	2.4	5.0	6.7	10
0.1–0.2	0.3–0.4	0.1–0.2	0.2–0.3	<0.1	0.2–0.3	0.2–0.3	0.1–0.2	0.1–0.2	0.2–0.3	0.2–0.3
15–25	35–45	15–25	25–35	<15	25–35	25–35	15–25	15–25	25–35	25–35
<b>31.6</b>	<b>62</b>	<b>37</b>	<b>43.25</b>	<b>25</b>	<b>34.6</b>	<b>40</b>	<b>35</b>	<b>38</b>	<b>41</b>	<b>50</b>
<b>IV</b>	<b>II</b>	<b>IV</b>	<b>III</b>	<b>IV</b>	<b>IV</b>	<b>IV</b>	<b>IV</b>	<b>IV</b>	<b>III</b>	<b>III</b>



unstable, ten are potentially unstable, seven are unstable at steeper cut slopes, and three are unstable (Fig. 4). The SMR results show good to very weak stability conditions (Table 2).

#### *Bhimphedi - Bhainsedobhan section*

Several large-scale instabilities were observed on the south-facing slope of the Mahabharat Range along the tributaries of the Rapti Khola (i.e. in the Mandu Khola and Rani Khola). Stability analyses were carried out at 18 sites, out of which one is stable, two are likely unstable, four are potentially unstable, three are unstable at steeper cut slopes, and eight are unstable (Fig. 5). The SMR results (Table 3) show that the slopes are fair at locations 293, 294, 341, 342, and 453, the stability conditions are weak at locations 271, 280, 283, 441, 452, and 34, and the conditions are very weak at locations 290, 440, and 451, whereas good stability conditions prevail at locations 271r and 275.

#### *Bhainsedobhan - Hetauda section*

Huge debris deposits were mapped along the upper reaches of the Khani Khola, Chandi Khola, Okhrenei Khola, Kalitar Khola, and Baghjhora Khola. Old as well as reactivated landslides are present at the source region of the Baghjhora Khola on highly fractured and disintegrated rock mass. Clay or talc infillings in the joints of the MT zone (i.e. in the Baghjhora watershed) further reduce the shear strength of the rock mass. Limestone mining and quarrying by the Hetauda Cement Factory at Kailash have disposed of a huge amount of debris in the nearby stream.

Out of the 22 analysed exposures, two are stable, six are likely unstable, four are potentially unstable, five are unstable at steeper cut slopes, and five are unstable (Fig. 6). The SMR results show good to weak stability conditions (Table 4).

### **BRIDGES ALONG THE MOST FEASIBLE ALIGNMENT**

Nine major bridges with a total length of 1,100 m are required for the most feasible alignment. They are:

1. Chitlang Khola Bridge No. 1 (100 m)
2. Chitlang Khola Bridge No. 2 (100 m)
3. Kulekhani Khola Bridge (100 m)
4. Lam Khola Bridge No. 1 (200 m)
5. Lam Khola Bridge No. 2 (100 m)
6. Mandu Khola Bridge (100 m)
7. Rani Khola Bridge (100 m)
8. Rapti River Bridge (150 m)
9. Samari Khola Bridge (150 m)

Besides the above bridges, a number of short bridges and/or culverts are also required to cross small tributaries. Surface engineering geological investigation of the bridge sites revealed that mostly fair quality of rock mass exists in the abutment sites of the bridges. The slope stability conditions of the abutment sites are also satisfactory,

provided suitable designs are made and pre-treatment to the foundation rock is carried out.

### **GEOTECHNICAL STUDY OF TUNNELS**

About 3.2 km long, 11 m wide, and 7.5 m high tunnel is proposed through the Chandragiri Hills to connect the Kathmandu Valley with the Chitlang Valley. The orientation of this proposed Thankot Tunnel is about 040°. Another tunnel named as the Kulekhani Tunnel has been proposed to connect the upper part of the Kulekhani Dam with its lower side. It is about 500 m long, 11 m wide, 7.5 m high, and trends due 172°. The last proposed tunnel crosses the Chisapani Hills of the Mahabharat Range and it is about 3.8 km long, 11 m wide, and 7.5 m high. It connects the Kulekhani Valley with the Rapti Valley and trends due 208°. Minor diversions on each tunnel may be necessary in order to get a safety factor of 1.5 (Broch 1984), which is based on the stability analysis of key blocks or rock wedges neglecting any influence of the stress regime. In view of the general stability of tunnels, the present study also takes into account the general theories of stability of tunnels including the finite element analysis (Witke 1990).

#### **Site geology**

The proposed Thankot Tunnel passes through limestone, mudstone, shale, and quartzite. Bedrock is expected below 20 m along the entire tunnel alignment. It encounters two local faults. The foliation is steeply dipping towards the south. The first part of the proposed Kulekhani Tunnel passes through massive marble beds and the remaining section is through thinly foliated micaceous quartzite of the Kulikhani Formation (Stöcklin and Bhattarai 1977). The foliation and bedding are dipping 28–45° due NE. The tunnel alignment is selected in such a way that it avoids the nearby Kulekhani Fault zone.

The first 1.1 km of the Chisapani Tunnel passes through granite with occasional schist bands. The next 1.3 km of the tunnel alignment runs through the Kulikhani Formation containing micaceous quartzite with intercalations of schist (Stöcklin and Bhattarai 1977). Further 0.7 km of the tunnel is in the white Chisapani Quartzite, and the remaining 0.7 km passes through the Kalitar Formation comprising schist alternating with quartzite. Six local faults (categorised as the second- and third-order discontinuities) are mapped along the Chisapani Tunnel alignment, but only four of them are expected to intersect the tunnel. The foliation is gently dipping in various directions. An anticline has been mapped near the southern portal of the Chisapani Tunnel.

#### **Rock mass**

The Chandragiri Formation consisting of medium- to thick-bedded limestone with the intercalation of chert and mudstone, and the Chitlang Formation represented by mudstone and shale with the intercalation of sandstone and calcareous bands are expected in the Thankot Tunnel. Medium- to thick-bedded marble alternating with thinly foliated phyllite (the Markhu Formation), and micaceous quartzite with the intercalation of schist (the Kulikhani

Formation) are expected along the Kulekhani Tunnel section. The Chisapani Tunnel encounters the Palung Granite, the Kulikhani Formation (medium- to thinly foliated quartzite with the intercalation of schist), and the white Chisapani Quartzite.

Four moderately spaced to close sets of discontinuity (i.e. a foliation or bedding joint set, two preferred joint sets, and one random joint set) are recorded at the surface along all the three tunnel alignments. The random set is not expected at the tunnelling depth except for the portals of the Thankot and Chisapani Tunnels, and along the Kulekhani Tunnel where the overburden is shallow. The discontinuity analyses show fair to very favourable tunnel orientation with respect to foliation or bedding, but unfavourable to very unfavourable orientation with respect to the major joint sets (Tables 5 and 6).

The rock mass expected along the three tunnels was classified on the basis of the data collected in the field, and the results are presented in Tables 7, 8, and 9.

**Stability analysis**

The Thankot and Chisapani Tunnels are divided into six geotechnical zones (viz., B, C, D, E, F, and G; Fig. 7 and 8), whereas the Kulekhani Tunnel is categorised into five geotechnical zones (viz., C, D, E, F, and G). The tunnelling

condition in zone B is good; it is fair in zones C and D, and weak in zones E and F, whereas it is critical in zone G (Humagain 1999). Based on the field data, the stability analysis of the proposed tunnels was carried out under the categories of structurally controlled, stress-controlled, weathering-controlled, and groundwater-controlled instability.

*Structurally controlled instabilities*

Based on the discontinuity data, the Thankot Tunnel alignment was divided into eight sections, the Kulekhani Tunnel into three sections, and the Chisapani Tunnel into 13 sections. The mean values of every joint set in each tunnel section were determined by the statistical analysis of the discontinuities using the computer program DIPS, whereas the stability analysis of key blocks and joint blocks was done using the computer program UNWEDGE (Tables 5 and 6; Fig. 9).

*Stress-controlled instabilities*

At a regional scale, the tectonic stress may be same in the three tunnels, as they all pass through the Kathmandu Nappe. However, the stress regime along a tunnel alignment may differ at local level due to the variation in depth, geology, geomorphology, tectonics, residual stress, time span, temperature, groundwater, and human behaviour. A considerable variation in the stress regime along the tunnel

**Table 5: Structural analysis of discontinuities in the Thankot Tunnel**

Ts. No. (Fig. 7)	Discontinuities	Tunnel faces and wedges							
		Roof			L Wall	R Wall	Floor	End Faces	
		1	2	3	4	5	6	NE	SW
1	Fp 53/195 J1 65/084 J2 69/324	Ro on J2	F	Ro on J1	S on J1-Fp	M S on J2-Fp	Stab	Ro. on Fp	ro. on J1-J2
2	Fp 57/198 J1 57/047 J2 85/123	F		Ro. on J2	M S on Fp-J1	Ro on J1-J2	Stab	Ro. on Fp-J2	Ro. on J1
3	Fp 58/195 J1 46/026 J2 69/103	F		Ro on J2	S on J2-J1	Ro on J1	Stab	Ro. on Fp	Ro. on J1-J2
4	Fp 47/186 J1 69/042 J2 70/302	Ro. on J2	F	Ro. on Fp	M S on Fp-J1	S. on J2-J1	Stab	M ro. on Fp-J2	Ro on J1
5	Fp 62/193 J1 71/289 J2 56/073	Ro. on J1	F	Ro. on Fp	M S on Fp-J2	M S on J1-J2	Stab	Ro. on J1-Fp	Ro on J2
6	Fp 50/175 J1 62/055 J2 61/317	S on J2	F	Ro. on J1	M S on J1-Fp	S on J2	Stab	M. Ro on Fp-J2	Ro. on J1
7	Fp 51/201 J1 58/051 J2 89/294	Ro. on J2	F	F + Ro. on Fp	M S on Fp-J1	Ro. on J1-J2	Stab	Ro on Fo-J2	Ro. on J1
8	Fp 38/203 J1 78/024 J2 79/120	F+Ro. on J1	F + Ro. on J2	Ro. on J2	S on J2-Fp		Stab	Ro. on Fp	Ro on J1-J2

**Abbreviations:** Ts. No: tunnel section number, Fp: foliation plane, J1, J2 and J3: joint set number. The other notations used for the mechanism of failure are F: falls from the excavation surface, S on: slides on, M S on: may slide on, Ro. on: rotates on, M ro. on: may rotates on, and Stab: stable.

Table 6: Structural analysis of discontinuities in the Chisapani Tunnel

Ts. No. (Fig. 8)	Discontinuities	Tunnel faces and wedges								Number of blocks
		Roof			L Wall	R Wall	Floor	End Faces		
		1	2	3	4	5	6	NE	SW	
1	Fp 30/048 J1 84/287 J2 77/161	Ro. on J2	F	Ro. on J1	M S on J1-Fp	M S on J2-Fp	Stab	Ro. on J1-J2	M ro. on Fp	6+2
	Fp, J2, J3 80/032	F	Ro. on J3	Ro. on J3-J2	M S on J2-Fp	Ro. on J3-Fp	Stab	Stab	Ro. on J2	6+2
	J1, J2, J3	Ro. on J2	F	Ro. on J1	Ro. on J1-J3	S on J2-J3	Stab	Ro. on J1-J2	Ro. on J3	6+2
2	Fp 52/070 J1 59/271 J2 87/014	F+S on Fp-J2	Ro. on J2	S. on J2-J1	S. on J2-J1	S on Fp-J2	Stab	M ro. on J1	Ro. on. Fp	5+2
3	Fp 32/030 J1 85/167 J2 84/088	Ro. on J2-J1	Ro. on J2	F	M S on J2-Fp	Stab	Stab	Ro. on J1	Ro. on Fp	6+2
4	Fp 51/097 J1 62/182 J2 87/146	S. on Fp	Ro. on J2	F+M S on J2-J1	M S on J2-J1	S. on Fp	Stab	Ro. on J1	Ro on Fp-J2	5+2
	Fp, J2, J3 52/010	S on Fp-J3	S on Fp-J3	S on Fp-J3	Stab	Stab	Stab	Stab	Ro. on J3-Fp	2+2
	J1, J2, J3	M S on J2-J3	Ro. on J2	F+M S on J2-J1	M S on J2-J1	M S on J2-J3	Stab	M ro. on J2-J1	M ro. on J2-J3	5+2
5	Fp 31/072 J1 90/305 J2 78/198	F	F	Ro. on J1	Ro. on J1-J2	M S on Fp-J2	Stab	Ro. on J1-J2	Ro on Fp	5+2
6	Fp 46/045 J1 65/175 J2 87/266	Ro on J1	F	Ro on J2	M S on J2-Fp	M S on J1-Fp	Stab	Ro. on J1-J2	Ro. on Fp	6+2
7	Fp 41/075 J1 88/324 J2 75/215	F	F	Ro. on J1	Ro. on J1-J2	S on Fp	Stab	Ro on J2	Ro. on J1-Fp	5+2
8	Fp 27/026 J1 79/113 J2 73/193	Ro. on J1	Ro. on J1+Fp	F+ S. on Fp		Stab	Stab	Ro. on J2	Ro. on J1-Fp	5+2
9	Fp 22/070 J1 51/226 J2 82/160	S on J2-Fp	Ro. on J2+F	S. on J2-J1	S. on J2-J1	S. on J2-Fp	Stab	Ro. on J1	Ro on Fp	5+2
	Fp, J2, J3 71/266	Ro. on J2	F	Ro. on J3	M. S on J3-Fp	S on J2-Fp	Stab	Ro. on J2-J3	Ro. on Fp	6+2
	J1, J2, J3	Ro. on J2	Ro. on J2-J3	S on J3	S. on J1-J2	M. S on J3-J1	Stab	Ro. on J2-J3	Stab	6+2
10	Fp 38/140 J1 77/254 J2 83/344	F	F+ Ro. on J1	Ro. on J1-J2		S on Fp	Stab	Ro. on J1	M. ro. on Fp-J2	5+2
11	Fp 54/132 J1 66/227 J2 52/349	S on Fp	F+Ro. on J1	M S on J1-J2	M S on J1-J2	S on Fp	Stab	Ro. on J1	M ro. on Fp-J2	5+2
12	Fp 44/135 J1 63/260 J2 81/017	Ro. on Fp	F	Ro. on J1	S. on J1-J2	S. on Fp-J2	Stab	Ro. on Fp	Ro. on J1-J2	6+2
13	Fp 54/156 J1 38/035 J2 74/334	S on J2-J1	F+ Ro. on J2	M. S. on J2-Fp	M. S. on J2-Fp	S. on J2-J1	Stab	M ro. on Fp-J2	Ro. on J1-J2	5+2
	Fp, J2, J3 81/264	1F+ S. on Fp	1F+ Ro on J3	Ro on J3+ 2F	M. S on J3-Fp	Stab	Stab	Ro. on Fp-J3	Ro. on J2	6+2
	J1, J2, J3	F	Ro. on J2	Ro. on J2-J3	M. S. on J3-J1	M. S on J2-J1	Stab	Stab	Ro. on J2	6+2

**Abbreviations:** Ts. No: tunnel section number, Fp: foliation plane, J1, J2 and J3: joint set number. The other notations used for the mechanism of failure are F: falls from the excavation surface, S on: slides on, M S on: may slide on, Ro. on: rotates on, M ro. on: may rotate on, and Stab: stable.

Table 7: 'Q' and RMR values for the Thankot Tunnel

Attribute	Location (as shown in Fig. 7)											
	T1	T2	T3	T4	T5	T6	T7	T8	T9	T10	T11	T12
'Q'	1.6	1.7	4.0	12.7	1.9	0.02	1.35	11.8	2.7	0.32	1.0	0.08
RMR = 9 ln Q + 44	48	49	56	67	50	10	47	66	53	13	44	22

Table 8: 'Q' and RMR values for the Kulekhani Tunnel

Attribute	Chainage, m			
	0 - 110	111 - 330	331 - 420	420 - 500
'Q'	0.83	8.9	1.8	0.53
RMR = 9 ln Q + 44	42	6.4	49	38

Table 9: 'Q' and RMR values for the Chisapani Tunnel

Attribute	Location (as shown in Fig. 8)														
	T1	T2	T3	T4	T5	T6	T7	T8	T9	T10	T11	T12	T13	T14	T15
'Q'	8.5	24	20	0.06	27	33	23	0.03	1.25	0.02	6.7	0.02	52	0.04	0.54
RMR = 9 ln Q + 44	63	73	71	18	74	75	72	12	46	9	61	10	80	15	38

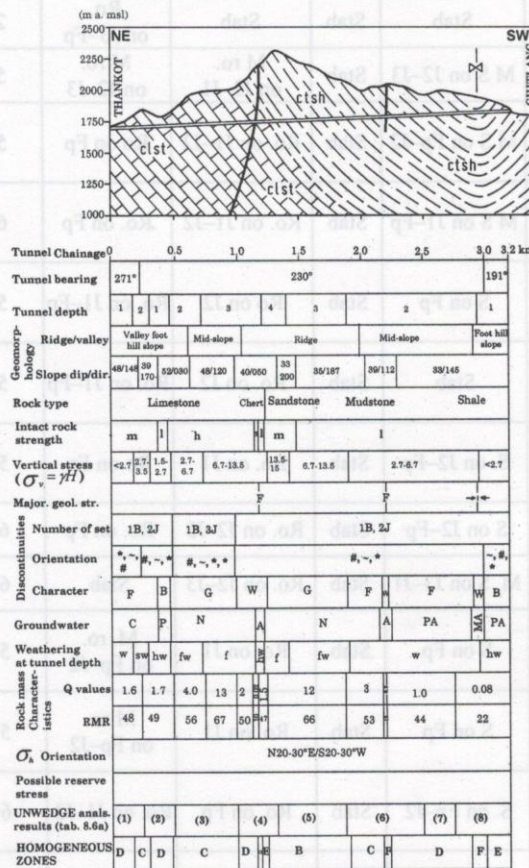


Fig. 7: Geotechnical zones along the Thankot Tunnel. Abbreviations: tunnel depth (1: <100 m, 2: 100–250 m, 3: 250–500 m, and 4: >500 m); intact rock strength (h: high, m: medium, l: low, and vl: very low); vertical stress in MPa; discontinuities (1B: bedding plane joint, 3J: three sets of preferred joint, \*: very unfavourable, -: unfavourable, ~: fair, +: favourable, #: very favourable, F: fair, B: bad, G: good, W: worse); Groundwater (N: negligible, C: considerable, PA: possibly active, A: active, and MA: more active); Weathering (w: weathered, sw: slightly weathered, hw: highly weathered, fw: faintly weathered, f: fresh)

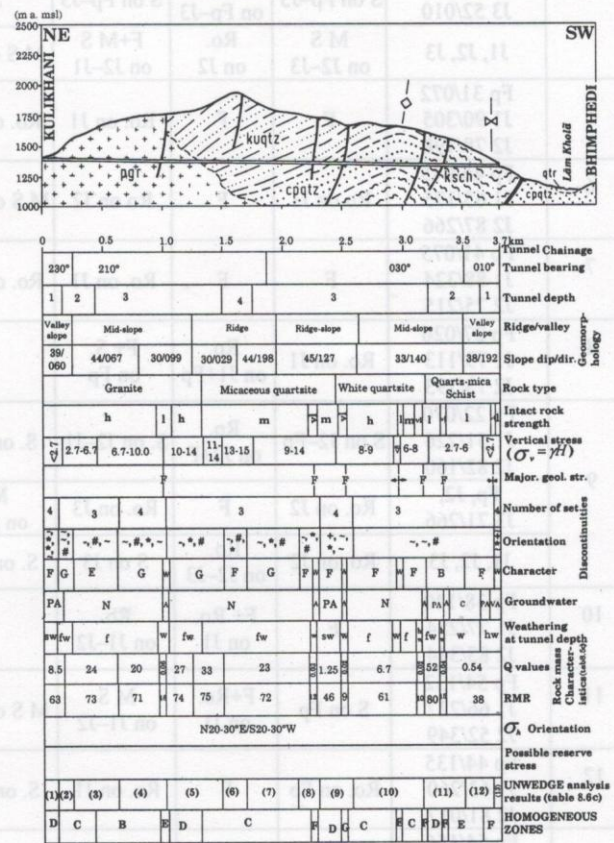


Fig. 8: Geotechnical zones along the Chisapani Tunnel. Abbreviations: tunnel depth (1: <100 m, 2: 100–250 m, 3: 250–500 m, and 4: >500 m); intact rock strength (h: high, m: medium, l: low, and vl: very low); vertical stress in MPa; discontinuities (1B: bedding plane joint, 3J: three sets of preferred joint, \*: very unfavourable, -: unfavourable, ~: fair, +: favourable, #: very favourable, F: fair, B: bad, G: good, W: worse); Groundwater (N: negligible, C: considerable, PA: possibly active, A: active, and MA: more active); Weathering (w: weathered, sw: slightly weathered, hw: highly weathered, fw: faintly weathered, f: fresh)

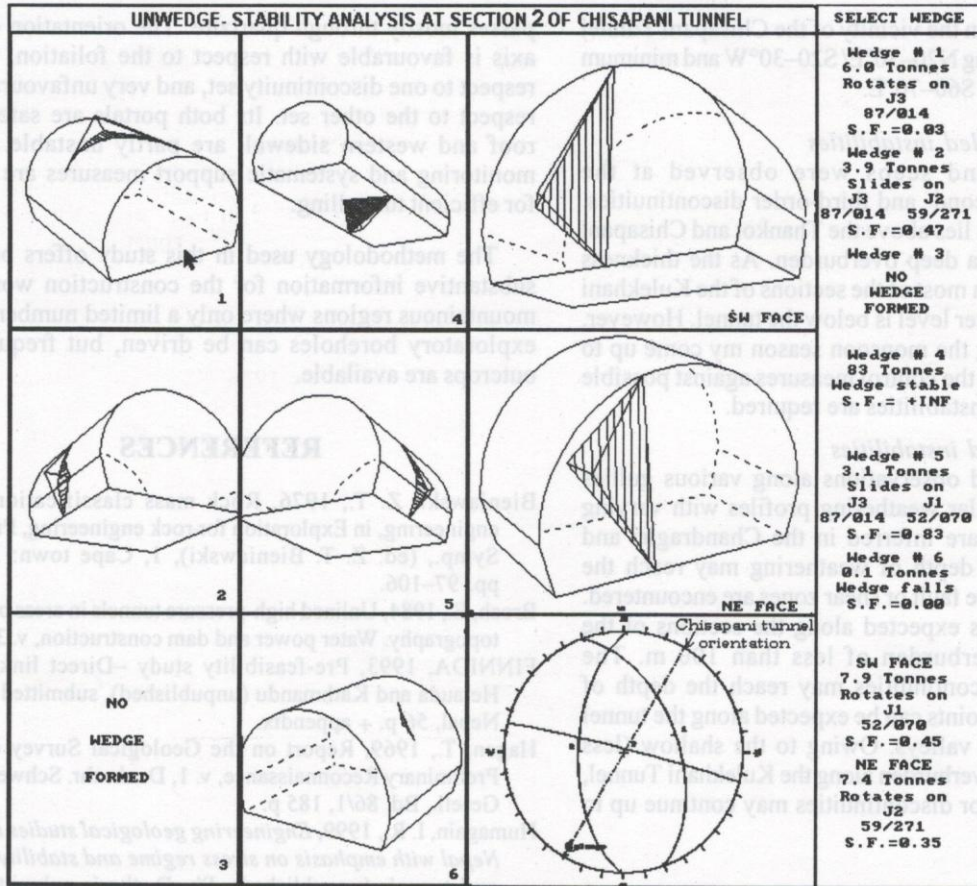


Fig. 9: Structurally controlled instabilities in the Chisapani Tunnel

length is expected due to the variation in the depth of overburden and mechanical parameters of rock mass as well as the presence of discontinuities and groundwater.

The state of stress in the Thankot and Chisapani Tunnels may also be influenced by the variation in the topography and the asymmetric distribution of the Chandragiri Hills and Mahabharat Range. Such influences are expected in the areas with the depth of overburden less than 250 m. The state of stress below the asymmetric ridges and corresponding valleys is also controlled by the directional anisotropy of rock as well as orientation and mechanical behaviour of discontinuities. The NNE-SSW directed compressive tectonic stress should also be added to get the total magnitude of the resultant principal horizontal stress on the excavation surfaces of the proposed tunnels. The topography and slope direction also affect the stress direction. A major stress decoupling at the boundary of the tectonic and topographical stresses as well as a shallow-level concentration of high stress is not expected in these tunnels.

Based on the stereographic analyses of the fourth- and fifth-order discontinuities, the principal stress directions of the proposed Thankot Tunnel alignment are found to be maximum ( $\sigma_1$ ) along N20-30°E/S20-30°W and minimum

( $\sigma_3$ ) along N60-70°W/S60-70°E. The tentative principal stress directions based on the fold axis of the syncline are the following: the  $\sigma_1$  acts along the NNE-SSW direction,  $\sigma_2$  is almost vertical (due to overburden) and  $\sigma_3$  acts along the WNW-ESE direction. If the direction of present-day principal horizontal stresses coincides with the direction determined by the discontinuity analysis, the axis of the Thankot Tunnel will be 10° to 20° oblique to the maximum horizontal stress.

The principal horizontal stress direction in the vicinity of the Kulekhani Tunnel was found to be maximum ( $\sigma_1$ ) along N20-40°E/S20-40°W and minimum ( $\sigma_3$ ) along N50-70°W/S50-70°E. Under these conditions, the axis of the tunnel will be 28° to 48° oblique to the maximum horizontal stress direction. Therefore, the tunnel orientation is slightly unfavourable. As this tunnel passes under the shallow overburden, the mechanical behaviour of rocks and topography play a major role in the stress regime. The marble and quartzite of the Kulekhani Tunnel alignment are of good quality and can withstand the unfavourable orientation. As the Chisapani Tunnel is almost parallel to the principal stress direction, a minimum adverse effect of horizontal stress is expected. Based on the stereographic analysis of the fourth- and fifth-order discontinuities, the tentative principal stress

directions of the area in the vicinity of the Chisapani Tunnel are: maximum ( $\sigma_1$ ) along N20–30°E/ S20–30°W and minimum ( $\sigma_3$ ) along N60–70°W/ S60–70°E.

#### Groundwater-controlled instabilities

Many springs and seeps were observed at the intersection of the second- and third-order discontinuities. The groundwater level lies above the Thankot and Chisapani Tunnels, which have a deep overburden. As the thickness of overburden is low in most of the sections of the Kulekhani Tunnel, the groundwater level is below the tunnel. However, the water table during the monsoon season may come up to the surface, and hence the control measures against possible groundwater-related instabilities are required.

#### Weathering-controlled instabilities

Based on the field observations along various gullies and tributaries, irregular weathering profiles with varying depth of weathering are inferred in the Chandragiri and Chisapani Hills. The depth of weathering may reach the tunnel in sections where fault or shear zones are encountered. The same condition is expected along the sections of the tunnels with the overburden of less than 100 m. The weathering along discontinuities may reach the depth of 200 m. Major release joints can be expected along the tunnel section close to deep valleys. Owing to the shallow (less than 200 m) depth of overburden along the Kulekhani Tunnel, weathering along major discontinuities may continue up to the tunnel alignment.

### CONCLUSIONS

The geotechnical investigations carried out along the most feasible alignment (i.e. the Thankot Tunnel–Chitlang Valley–Kulekhani Valley– Kulekhani Tunnel–Chisapani Tunnel–Bhimphedi–Bhainsedobhan–Hetauda) have revealed that 60–75% of the total road length is stable, 20–30% is fair, 5–15% is weak, and 2–5% is critical. Relatively better stability conditions are expected along the most feasible alignment. However, a few instabilities are expected in critical areas.

The Thankot Tunnel passes through quartzite, phyllite, and limestone. Its orientation is fair to very favourable with respect to the foliation or bedding, but unfavourable with respect to the major discontinuity sets. Its two portals, roof, and sidewalls are partly unstable. The Kulekhani Tunnel runs mostly through marble bands. Its two portals and roof as well as sidewalls are also partly unstable. The northern portal of the Chisapani Tunnel is in granite, but the tunnel

passes mostly through quartzite. The orientation of tunnel axis is favourable with respect to the foliation, fair with respect to one discontinuity set, and very unfavourable with respect to the other set. Its both portals are safe, but the roof and western sidewall are partly unstable. Regular monitoring and systematic support measures are required for efficient tunnelling.

The methodology used in this study offers better and substantive information for the construction work in the mountainous regions where only a limited number of or no exploratory boreholes can be driven, but frequent rock outcrops are available.

### REFERENCES

- Bieniawski, Z. T., 1976, Rock mass classification in rock engineering, in Exploration for rock engineering, Proc. of the Symp., (ed. Z. T. Bieniawski), 1, Cape town: Balkema, pp. 97–106.
- Broch, E., 1984, Unlined high-pressure tunnels in areas of complex topography. Water power and dam construction, v. 36, no. 11.
- FINNIDA, 1993, Pre-feasibility study –Direct link between Hetauda and Kathmandu (unpublished), submitted to HMG/ Nepal, 56 p. + appendix.
- Hagen, T., 1969, Report on the Geological Survey of Nepal, Preliminary Reconnaissance, v. 1, Denkschr. Schweiz Naturf. Gesell., Bd. 86/1, 185 p.
- Humagain, I. R., 1999, *Engineering geological studies in Central Nepal with emphasis on stress regime and stability of slopes and tunnels* (unpublished), Ph. D. thesis submitted to the Aachen University of Technology, Germany, 333 p.
- Romana, M., 1985, New adjustment rating for application of Bieniawski classification to slopes. In Proc. of Int. Symp. Rock Mech. Excav. Min. Civ. Works. ISRM, Mexico City, pp. 59–68.
- Stöcklin, J., 1980, Geology of Nepal and its regional frame, Jour. Geol. Soc., v. 137, London, UK, pp. 1–34.
- Stöcklin, J. and Bhattarai, K. D., 1977, Geology of Kathmandu area and Central Mahabharat Range, Nepal Himalaya, HMG/ UNDP Mineral Exploration Project, Technical report, DP/ UN/NEP-73-019/3, 86 p., (unpublished).
- Upreti, B. N. and Le Fort, P., 1997, Lesser Himalayan Crystalline Nappes of Nepal: Problem of their origin, Geol. Soc. Am. Bull. (Special paper 328), 1999, pp. 225–238.
- Wagner, A. A., 1957, The use of the Unified Soil Classification System by the Bureau of Reclamation, Proc. 4th Inter. Conf. Soil Mech. Found. Eng. (London), v. 1, 125 p.
- Witke, W., 1990, *Rock mechanics: theory and applications with case histories*, translated by Sykes, R., Springer-Verlag, 1076 p.